Drug Design, Development and Therapy

Dovepress
Taylor & Francis Group

Open Access Full Text Article

ORIGINAL RESEARCH

Design, Synthesis and Antiproliferative Activity Studies of Novel 1,2,3-Triazole-Urea Hybrids

En Gao[1,2], Haoying Zhang[1], Yajie Guo[3], Xi Wang[1], Longfei Mao[4], Lizeng Peng[5], Guiqing Xu[1], Xiaojun Yao[2], Shouhu Li[6], Huibao Long[3], Tong Wang[3], Haidong Wu[3]

[1]School of Chemistry and Chemical Engineering, Henan Normal University, Xinxiang, 453000, People's Republic of China; [2]State Key Laboratory of Quality Research in Chinese Medicine/Macau Institute for Applied Research in Medicine and Health, Macau University of Science and Technology, Macau, People's Republic of China; [3]Department of Emergency, the Eighth Affiliated Hospital, Sun Yat-Sen University, Shenzhen, 518033, People's Republic of China; [4]College of Basic Medicine and Forensic Medicine, Henan University of Science and Technology, Luoyang, 471003, People's Republic of China; [5]Institute of Agro-Food Science and Technology, Shandong Academy of Agricultural Sciences, Jinan, 250100, People's Republic of China; [6]School of Pharmacy, Xinxiang University, Xinxiang, Henan, 453000, People's Republic of China

Correspondence: En Gao, School of Chemistry and Chemical Engineering, Henan Normal University, Xinxiang, 453000, People's Republic of China, Email ge_163@126.com; Lizeng Peng, Shandong Academy of Agricultural Sciences, 202 Gongye North Road, Licheng District, Jinan City, 250000, People's Republic of China, Email penglizeng@sdnu.edu.cn

Introduction: The development of novel targeted therapies for hepatocellular carcinoma remains a critical need in oncology. This study aimed to design and evaluate a new series of triazole-urea hybrid compounds for their anti-cancer potential.

Methods: A series of urea compounds bearing terminal alkynyl groups were synthesized *via* an assembly and post-modification strategy. Subsequent Click chemistry yielded the novel triazole-urea hybrids (**3a**–**3e**, **5a**–**5e**, **7a**–**7e**). Their anti-proliferative effects were assessed against multiple human cancer cell lines (lung: H460, H1299, A549, PC-9; liver: Huh-7; breast: MCF-7) and normal liver cells (L02) using the CCK-8 assay. Mechanisms were investigated through apoptosis, autophagy, and DNA damage assays. An acute oral toxicity study was conducted in female KM mice at a dose of 500 mg/kg, with thorough monitoring of body weight, organ coefficients, and histopathology of major organs.

Results: Most compounds exhibited potent, concentration- and time-dependent anti-proliferative activity against Huh-7 liver cancer cells, with only marginal effects on other tested cancer lines. Crucially, no cytotoxicity was observed in normal L02 cells. Mechanistic studies revealed that the lead compound induced apoptosis, autophagy, and DNA damage in Huh-7 cells. The in vivo assay demonstrated no drug-related mortality or significant adverse effects on body weight, organ coefficients, or histology at 500 mg/kg over 14 days, indicating a high maximum tolerated dose and an excellent preliminary safety profile.

Conclusion: These findings demonstrate the selective anti-liver cancer efficacy and favorable in vivo safety of these triazole-urea hybrids, particularly compound **3c**, underscoring their strong potential as promising therapeutic candidates for hepatocellular carcinoma.

Keywords: 1,2,3-triazoles, urea, hepatic cancer, anticancer activity

Introduction

Cancer remains a leading cause of global morbidity and mortality, with drug resistance posing a critical barrier to therapeutic efficacy.[1,2] China has a significant number of cancer patients and ranks first in the world for cancer mortality. In 2020, cancer accounted for approximately 9.96 million deaths worldwide, of which 30% occurred in China, underscoring the urgent need for innovative treatment strategies.[3] While multifactorial mechanisms drive therapeutic failure, chemoresistance significantly limits the clinical utility of conventional therapies.[4,5] This challenge necessitates the development of novel agents with distinct mechanisms to circumvent resistance pathways.[6]

For many years, 1,2,3-triazoles have served as a rich source of inspiration for medicinal chemists, primarily due to their ability to be synthesized through click chemistry and their possession of a diverse array of biological activities.[7] 1,2,3-Triazole is a versatile fragment present in numerous bioactive molecules, including antifungal, antibacterial, antiallergic, anti-HIV, antituberculosis, and anti-inflammatory agents.[7] In recent years, there has been a surge of interest

Received: 5 June 2025
Accepted: 3 October 2025
Published: 22 October 2025

in investigating the pharmacological effects of 1,2,3-triazole. It is anticipated that this compound, when conjugated with a wide range of groups, will play a pivotal role in the design of anticancer drugs.[8,9]

Triazole is a common five-membered aromatic heterocyclic structure, characterized by weak basicity and two isomers: 1,2,3-triazole and 1,2,4-triazole. The nitrogen atom in triazole can function as a hydrogen bond acceptor, while the NH group can serve as a hydrogen bond donor, facilitating interactions with biological targets. Due to the difference in electronegativity between carbon and nitrogen, triazoles exhibit polarity, which results in a lower logP value, potentially enhancing the water solubility of compounds. Furthermore, the metabolism of triazoles is relatively stable.[10]

The urea moiety is widely exploited in drug design for its ability to modulate target engagement and optimize physicochemical properties.[11] Urea-containing compounds demonstrate enhanced selectivity and metabolic stability, making them valuable frameworks for addressing drug resistance.[12] Molecular hybridization refers to the covalent combination of two or more drug pharmacophores into a single molecule.[13] This approach serves as an effective tool for designing highly active new entities.[14] The resulting combined pharmacophores can target multiple therapeutic pathways, thereby providing opportunities to circumvent resistance.[15] This strategy enables synergistic effects while minimizing unwanted side effects, as evidenced by recent advances in antitumor drug discovery.[16]

The molecular hybridization strategy, which integrates distinct pharmacophores into single molecules, has garnered significant attention in anticancer drug discovery. Recently, Haval et al designed and synthesized novel quinoline–1,2,3-triazole hybrids via copper-catalyzed azide-alkyne cycloaddition (CuAAC).[17,18] Among them, multiple compounds demonstrated potent anti-proliferative activity against MCF-7 cells, with IC_{50} values as low as 0.39 μg/mL, surpassing doxorubicin. These hybrids also exhibited favorable drug-likeness, ADMET properties, and strong CDK2 binding, supported by DFT and docking studies, underscoring their potential as kinase-targeting anticancer agents. Significant precedents support this approach: Liu et al developed a range of innovative 1,2,3-triazole-pyrimidine-urea hybrids (Figure 1, I) with effective antitumor ability against four different tumor cell lines: MGC-803, EC-109, MCF-7, and B16-F10. Of particular interest, one compound demonstrated a noteworthy inhibitory effect on B16-F10, yielding an IC_{50} value of 32 nM, inducing concentration-dependent apoptosis.[19] The compound reported by Sanofi (Figure 1, II) emerges as an efficacious and highly selective inhibitor of the MET receptor tyrosine kinase (RTK), demonstrating nanomolar inhibition (IC_{50} = 4.2 nM) and selective cytotoxicity in MET-amplidied tumors.[20] The ABHD6 inhibitor piperidinyl 1,2,3-triazourea (Figure 1, III), designed by Cravatt's research group, achieves cellular degradation at nanomolar concentrations, with KT185 showing exceptional in vivo selectivity.[21] Liu's research group further reported 1,2,3-triazole-dithiocarbamate-urea hybrids (Figure 1, IV) exhibiting broad-spectrum activity (IC_{50} values of compounds IVa and IVb ranging from 1.62 to 20.84 μM and 0.76 to 13.55 μM, respectively).[22] The IDO1 inhibitor devised by Mao

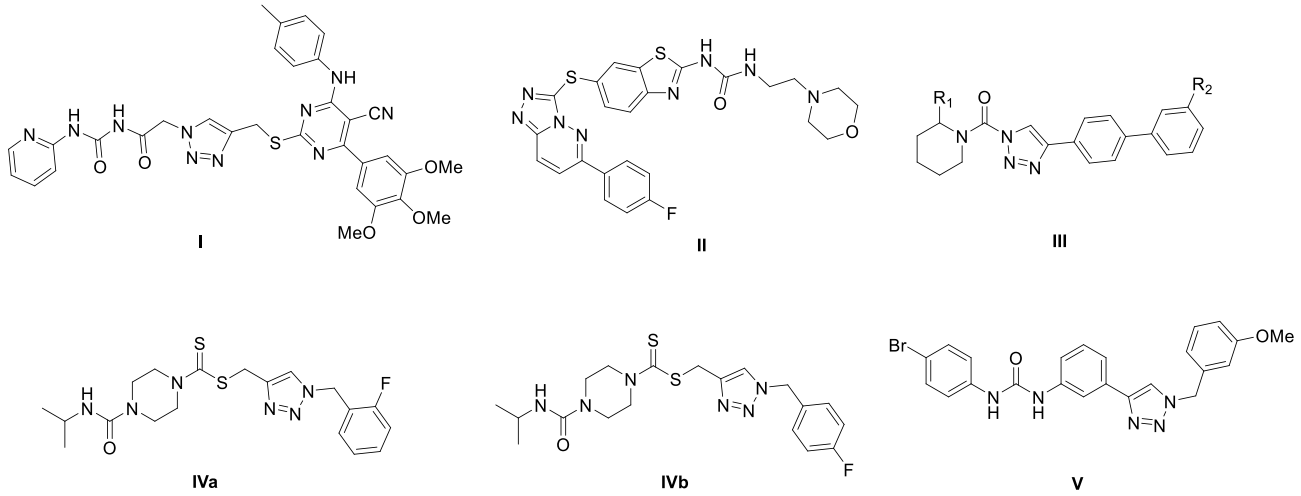

Figure 1 The structures of 1,2,3-triazole urea hybrids.

represents a targeted compound achieved through the synthesis of urea with a 1,2,3-triazole structure (Figure 1, V), demonstrating potent enzymatic inhibition (IC_{50} = 0.75 μM) through optimized target binding.[23]

Although the aforementioned 1,2,3-triazole-containing scaffolds show great promise in targeted therapy, most of them focus on optimizing potency against a single target. To more effectively address the complex mechanisms of tumor drug resistance, we aimed to develop novel hybrid molecules with potential for multimodal action. In this study, we report for the first time a new chemical entity that rationally couples the 1,2,3-triazole motif with a urea functional group. The urea group was chosen due to its role as a privileged structure in numerous bioactive molecules and its capacity to form strong hydrogen-bonding interactions with biological targets. We hypothesized that this unique hybridization strategy would yield synergistic effects, potentially overcoming resistance to existing therapies (eg, pure triazole-based inhibitors) and enhancing antitumor efficacy through simultaneous engagement with multiple targets.

Building on our previous work with gefitinib-1,2,3-triazole derivatives demonstrating broad-spectrum anticancer activity,[24,25] we hypothesize that merging 1,2,3-triazole with urea motifs could yield synergistic effects against resistant malignancies. Herein, we report the design, synthesis, and evaluation of novel triazole-urea conjugates targeting drug-resistant cancers. Our systematic investigation reveals their selective antiproliferative effects against hepatocellular carcinoma via multimodal mechanisms, supported by in vivo safety profiles.

Chemistry

Based on previous studies,[23,24] we successfully designed and synthesized a series of novel compounds incorporating 1,2,3-triazole structure and a urea moiety. Three types of functional groups (m-phenyl group, p-phenyl group, and methyl group) were selected as linkers to connect urea and 1,2,3-triazole blocks, respectively. The reaction routes of the three series of compounds (**3a-3e**, **5a-5e**, **7a-7e**) are shown in Figure 2 and Table 1. Different substituents (R_1, R_2, R_3, R_4 and R_5) were present on the benzene ring of phenyl isocyanate and benzyl structures. The effects of linker substituents R_1, R_2, R_3, R_4 and R_5 on selected human tumor cell lines were compared.

Results and Discussion

Effects of Compounds 3a-3e, 5a-5e, and 7a-7e on Tumor Cell Viability and Cytotoxicity

To evaluate the anti-tumor potential of the newly synthesized compounds, we treated different types of human tumor cell lines (lung cancer cell lines H460, H1299, A549, and PC-9, hepatocellular carcinoma cell line Huh-7, and breast cancer

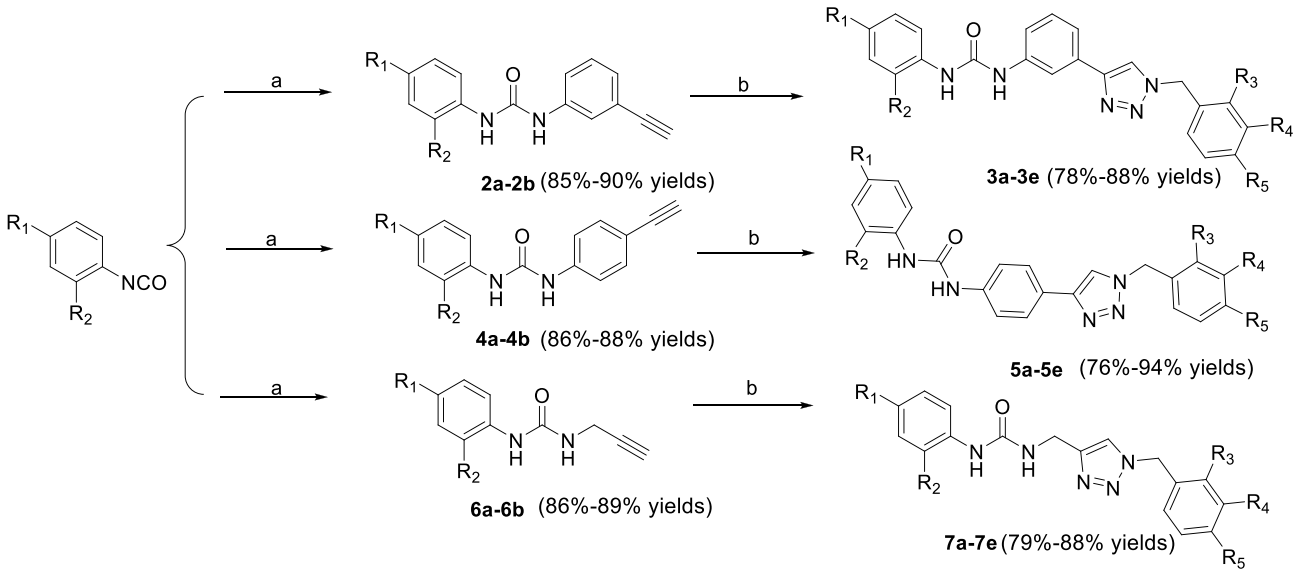

Figure 2 The reaction routes to compounds **3a-3e**, **5a-5e**, and **7a-7e**.

https://doi.org/10.2147/DDDT.S536920

Table 1 R-Group of Compounds **3a-3e**, **5a-5e**, and **7a-7e**

Compound	R_1	R_2	R_3	R_4	R_5
3a	Cl	H	H	H	Cl
3b	Cl	H	H	Cl	H
3c	Cl	H	H	H	Br
3d	H	Br	H	H	Cl
3e	H	Br	H	H	Br
5a	Cl	H	H	H	Cl
5b	Cl	H	H	Cl	H
5c	Cl	H	H	H	Br
5d	H	Br	H	H	Cl
5e	H	Br	H	H	Br
7a	Cl	H	H	H	Cl
7b	Cl	H	H	Cl	H
7c	Cl	H	H	H	Br
7d	H	Br	H	H	Cl
7e	H	Br	H	H	Br

cell line MCF-7) with 20 μM or 50 μM concentrations, using L02 normal liver cells as a control cell line. Cell viability was assessed after 48h or 72h using the CCK-8 assay in Table 2.

Compounds **3a-3e** demonstrated significant antiproliferative activity against Huh-7 cells at a concentration of 50 μM following 72 hours of treatment. Notably, these compounds induced substantially higher inhibition rates in Huh-7 cells compared

Table 2 Cell Viability and Cytotoxicity of Compounds **3a-3e**, **5a-5e**, and **7a-7e** on Human Lung Cancer Cell Lines

Compound	H460	H1299	A549	A549	PC-9	PC-9
	50μM, 72h	**50μM, 72h**	**50μM, 72h**	**20μM, 72h**	**50μM, 72h**	**20μM, 72h**
3a	72.03±1.93	76.26±14.26	101.44±1.93	121.39±6.44	110±6.52	95.40±1.83
3b	88.71±1.56	103.60±10.83	166.34±4.24	114.55±8.33	117.63±3.89	102.16±7.50
3c	61.39±0.78	76.66±8.20	122.92±7.18	108.07±9.57	127.63±5.02	85.97±4.11
3d	65.29±5.19	130.33±1.08	148.92±25.57	158.77±16.71	107.37±6.27	130.28±4.98
3e	46.74±4.50	108.25±3.15	70.94±5.81	130.05±3.43	92.63±1.47	127.79±2.24
5a	86.32±5.28	88.13±2.37	79.61±3.83	73.16±3.26	81.30±2.01	85.98±5.69
5b	69.30±1.45	82.80±0.23	73.15±1.94	64.62±1.69	76.41±1.82	72.06±1.23
5c	82.21±0.89	89.87±3.30	78.81±1.42	69.12±0.72	80.44±2.54	71.50±1.22
5d	74.93±4.42	109.33±2.15	106.75±1.22	102.47±1.57	102.88±2.78	98.31±5.01

(*Continued*)

Table 2 (Continued).

Compound	H460	H1299	A549	A549	PC-9	PC-9
	50μM, 72h	50μM, 72h	50μM, 72h	20μM, 72h	50μM, 72h	20μM, 72h
5e	81.40±4.92	115.33±2.93	88.98±3.16	77.29±3.08	105.94±9.45	85.04±3.34
7a	73.19±0.35	82.27±4.39	67.63±2.98	61.69±2.21	81.69±3.31	83.16±0.73
7b	88.46±2.41	91.60±1.62	79.54±5.81	76.69±6.46	90.03±4.17	90.87±3.42
7c	87.65±1.38	91.47±0.67	96.99±4.42	102.40±4.84	178.62±5.90	111.19±3.96
7d	61.61±5.53	90.67±1.50	86.07±2.46	86.36±1.03	126.75±10.69	94.54±0.43
7e	63.39±2.15	89.20±0.83	91.51±1.83	88.83±1.55	162.70±5.67	99.25±0.66
5-FU	35.30±1.58	32.54±0.87	28.12±0.73	35.36±1.63	32.07±1.37	48.49±0.19

to the control group, indicating potent growth-inhibitory effects. In contrast, minimal cytotoxic effects were observed in MCF-7 and L02 cells under identical experimental conditions, suggesting selective targeting of Huh-7 cells by these derivatives.

When compared to the positive control drug 5-FU under identical experimental conditions (50 μM, 72-hour exposure), 5-FU exhibited significantly weaker antiproliferative activity against Huh-7 cells. Quantitative assessment of data presented in Table 3 reveals that these derivatives achieved statistically higher inhibition rates compared to 5-FU across multiple cancer cell

Table 3 Cell Viability and Cytotoxicity of Compounds **3a-3e**, **5a-5e**, and **7a-7e** on Huh-7, MCF-7, and L02

Compound	Huh-7		MCF-7		L02
	50μM, 48h	50μM, 72h	50μM, 48h	50μM, 72h	50μM, 72h
3a	84.05±6.96	15.60±4.19	103.82±0.52	98.15±0.33	101.53±3.20
3b	73.71±2.02	14.99±1.74	92.31±3.39	70.47±2.18	71.79±2.49
3c	60.53±1.40	13.09±2.47	96.54±1.02	86.79±3.30	97.38±3.01
3d	53.11±0.76	11.16±0.22	89.47±2.26	69.62±0.48	62.19±5.21
3e	61.25±2.65	10.79±0.38	89.74±0.40	76.79±0.96	45.21±3.98
5a	83.63±5.51	72.81±6.41	94.60±0.95	97.98±0.53	109.78±3.32
5b	86.69±3.72	70.37±1.73	91.80±0.13	98.20±3.54	92.59±0.66
5c	98.39±2.16	64.97±1.20	93.68±1.32	97.83±1.52	107.35±1.40
5d	80.25±6.13	87.22±4.09	99.33±2.76	104.30±0.28	112.55±11.33
5e	70.79±4.40	72.81±2.87	92.90±0.55	103.16±2.23	103.80±0.11
7a	65.70±0.65	60.49±2.19	80.75±2.83	83.30±1.25	126.60±11.54
7b	86.07±6.06	82.18±7.45	82.00±2.22	87.20±2.91	99.97±2.81
7c	88.20±4.82	87.88±1.35	89.80±2.64	91.17±1.78	140.67±2.81
7d	66.27±1.56	65.58±0.22	84.41±1.62	88.63±0.38	117.25±0.76
7e	61.23±3.60	72.91±1.03	84.69±0.91	80.24±1.24	106.98±0.44
5-FU	50.52±2.38	44.39±1.48	96.45±1.20	88.13±0.71	98.98±2.09

https://doi.org/10.2147/DDDT.S536920

models, with Huh-7 cells demonstrating the most pronounced differential response. These findings collectively validate the compounds' enhanced selectivity and efficacy in targeting hepatocellular carcinoma cells.

The half-maximal inhibitory concentrations (IC_{50}) of the tested compounds against Huh-7 cells were determined following a 72-hour exposure period. Cell viability was quantified using CCK-8 assay after incubation with serial dilutions of each compound. Growth inhibition percentages were calculated from viability data, and IC_{50} values were subsequently derived through nonlinear regression analysis of dose–response curves. These results including statistical parameters are comprehensively summarized in Table 4.

The IC_{50} values for compounds **3a-3e** against Huh-7 cells were mostly below 15 μM, with compound **3c** exhibiting the highest activity (IC_{50} = 10.23 ± 1.32 μM) and compound **3e** exhibiting the highest activity (IC_{50} = 12.25±1.31 μM). In contrast, compounds **5a-5e** and **7a-7e** displayed IC_{50} values exceeding 50 μM. These findings suggest that the m-phenyl linker between the urea and triazole moieties confers superior activity compared to p-phenyl or methyl linkers.

To further evaluate the impact of different linking groups on activity, we selected compounds with identical substituents on the left and right benzene rings for comparison. Subsequently, the compounds (ie, **3a**, **5a** and **7a**; **3b**, **5b** and **7b**; **3c**, **5c** and **7c**; **3d**, **5d** and **7d**; **3e**, **5e** and **7e**) were compared to ascertain that the m-phenyl linker is the preferred substituent in terms of enhancing inhibitory activity.

Additionally, the positive control 5-FU exhibited an IC_{50} value of 38.98 ± 0.56 μM, further corroborating the superior activity of compounds **3a-3e**. This comparison not only validates the advantage of the m-phenyl linker but also emphasizes the high efficacy of compounds **3a-3e** when benchmarked against the positive control. These results provide valuable insights for future drug design, particularly in selecting linkers to enhance compound activity.

Anti-Cell Proliferation Effects of Compounds 3c and 3e Against Huh-7 Cells

To further explore the anti-proliferation effects of compounds **3c** and **3e**, we performed the live and dead cell staining assay by using the Calcein Acetoxymethyl Ester (Calcein-AM) and Propidium Iodide (PI) dyes. Living cells stained by Calcein-AM and showed green fluorescence, while dead cells will stain with red fluorescence by PI. We seeded Huh-7 cells in a 96 well plate and treated them with different concentrations (5, 10, 20 μM) of compound **3c** and **3e**, respectively. After 24h treatment, Calcein-AM and PI were added to cells and stained for one hour in dark, then the cells were observed under a fluorescence confocal microscopy. Results are shown in Figure 3. After treatment, dead cells were increased significantly in a dose-dependent manner, while live cells were decreased. This result suggested that the compounds **3c** and **3e** had effective anti-proliferation abilities against Huh-7 cells.

Effects of Compounds 3c and 3e on Cell Apoptosis

Apoptosis is a cell self-destruction process that can lead to cell death. To further investigate the effects of compounds **3c** and **3e** on cell apoptosis, we treated Huh-7 cells with different concentrations (5, 10, 20 μM) of **3c** and **3e** for 72h, respectively. After treatment, cells were digested, collected and stained with Annexin V-FITC and PI. Samples were then detected and analyzed using the flow cytometry to evaluate the apoptotic cells. The necrotic cells (Q1, AV-/PI+), late apoptotic cells (Q2, AV+/PI+), early apoptotic cells (Q3, AV+/PI-), and live cells (Q4, AV-/PI-) were calculated. Results revealed dose-dependent increases in apoptotic cells after 3c and 3e treatment (Figure 4A and B).

Table 4 IC_{50} Values of Designed Derivatives Against Huh-7 Cells

Compd No.	IC_{50} (μM)	Compd No.	IC_{50} (μM)	Compd No.	IC_{50} (μM)
	Huh-7		Huh-7		Huh-7
3a	13.04±0.10	**5a**	>50	**7a**	>50
3b	15.13±0.09	**5b**	>50	**7b**	>50
3c	10.23±1.32	**5c**	>50	**7c**	>50
3d	13.50±0.59	**5d**	>50	**7d**	>50
3e	12.25±1.31	**5e**	>50	**7e**	>50
5-FU	38.98±0.56				

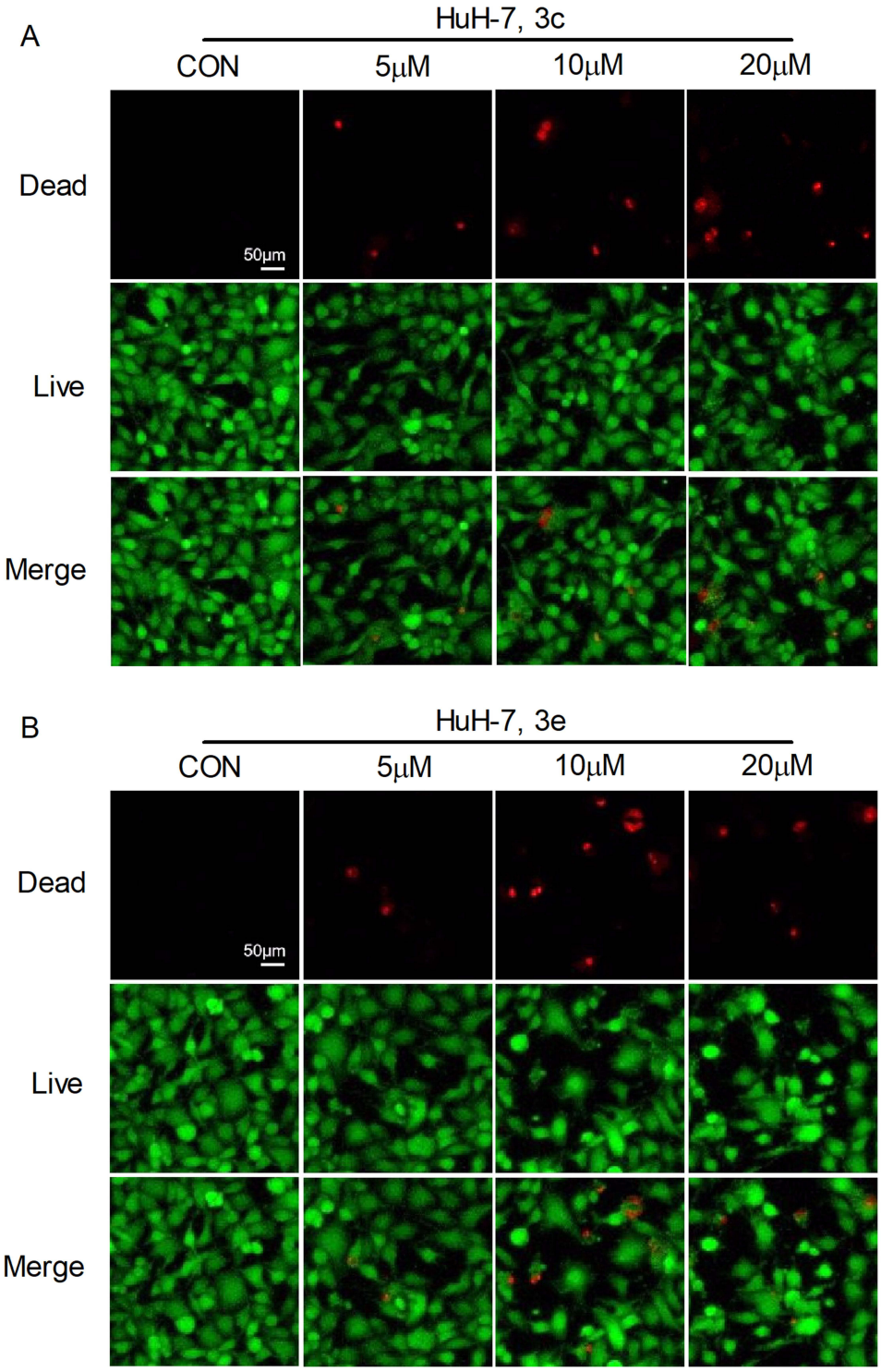

Figure 3 Dead and living cells staining. (**A**) Fluorescence image of Huh-7 cells treated with compound **3c** for 24 h. (**B**) Fluorescence image of Huh-7 cells treated with compound **3e** for 24 h. n = 5–6.

Effects of Compounds 3c and 3e on Gene Expression Related to Cell Death

In order to investigate the molecular mechanisms of compounds **3c** and **3e** on cell death and cell proliferation, we treated Huh-7 cells with 10 μM of **3c** and **3e** and detected the expressions of key genes related to cell growth and death processes, including DNA damage, oxidative stress, apoptosis, and autophagy. After 72 h treatment, cells were collected

https://doi.org/10.2147/DDDT.S536920

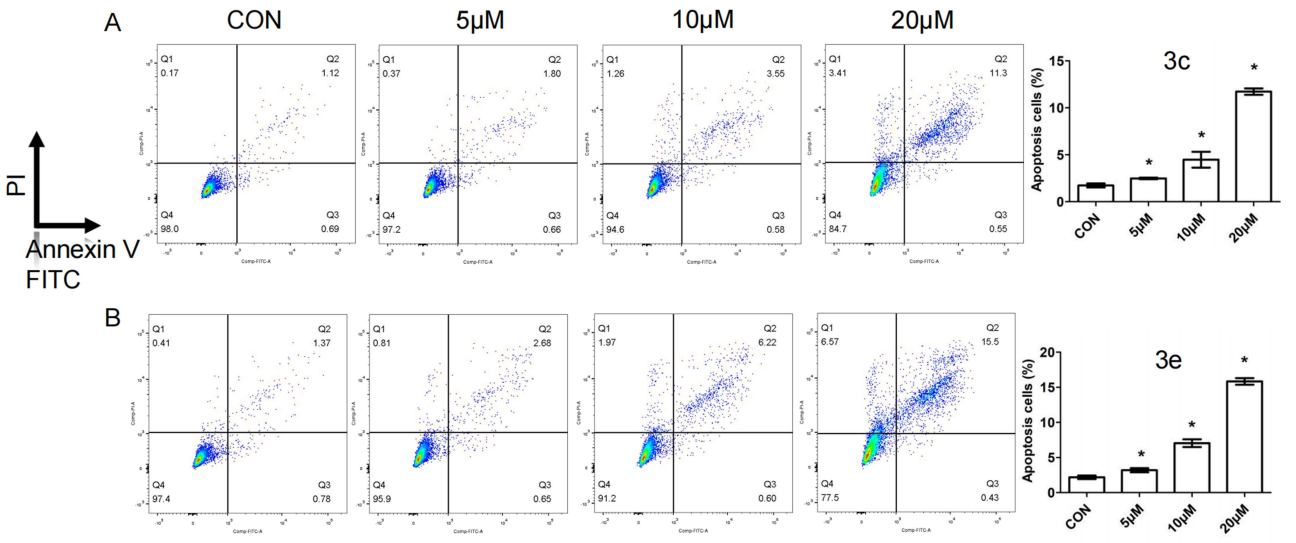

Figure 4 Cell apoptosis measurement. (**A**) Huh-7 cells were treated with 5 μM, 10 μM or 20 μM of compound **3c** for 72 h and apoptotic cell distribution was detected. (**B**) Huh-7 cells were treated with 5 μM, 10 μM or 20 μM of compound **3e** for 72 h and apoptotic cell distribution was detected. Data are presented as Mean ± SE. Significant differences were assessed by one-way ANOVA followed by Dunnett's tests. *P<0.05. n = 5.

and analyzed by RT-PCR. Results showed that compound **3c** upregulated the expression of Keap1, which was an important gene involved in oxidative stress although the other oxidative stress genes such as Nrf2, Gpx4, and TNFa had no significant changes (Figure 5A). Besides, **3c** treatment did not influence the expressions of DNA damage-related genes p53, p21, and H2AX, apoptosis-related genes Bcl2, caspase6, and caspase7, autophagy genes ATG5 and ATG7

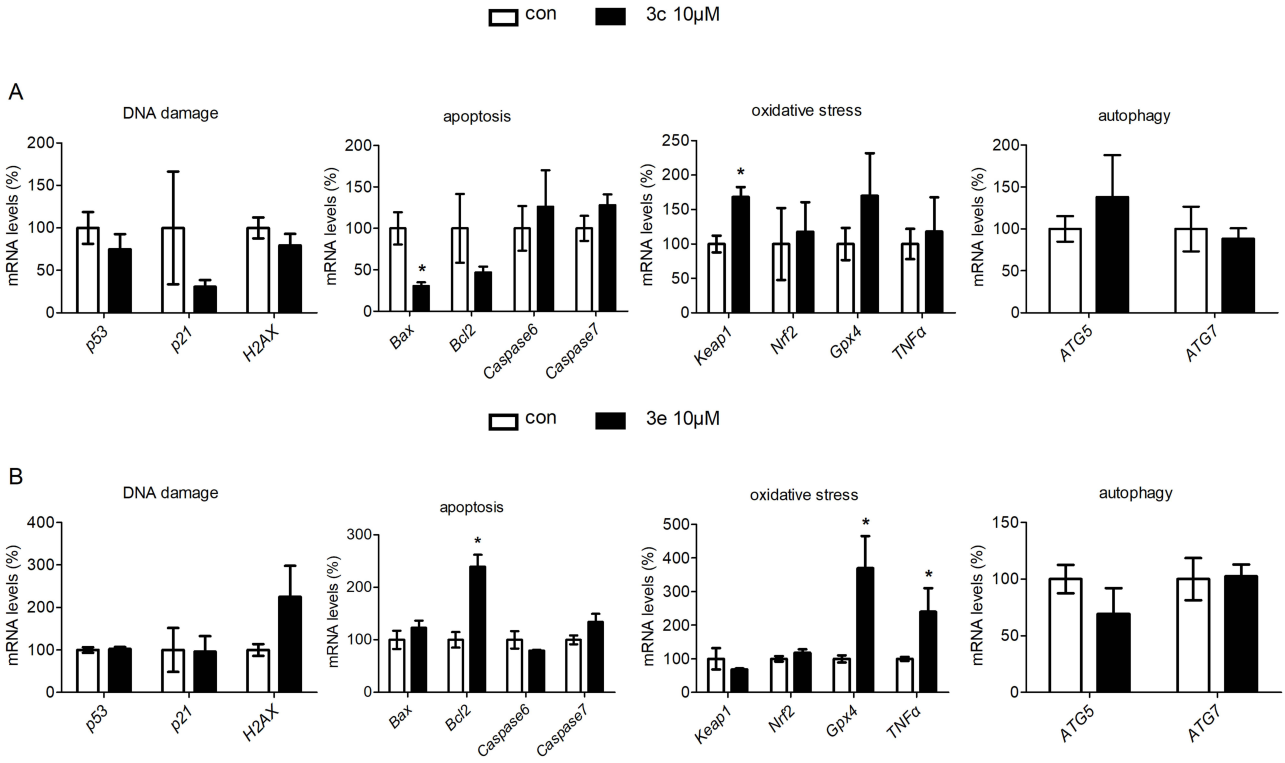

Figure 5 Gene expression analysis. (**A**) P53, P21, H2AX, Bax, Bcl2, caspase6, caspase7, Keap1, Nrf2, Gpx4, TNFa, ATG5, ATG7 mRNA levels of compound **3c** treated Huh-7 cells for 72h. (**B**) P53, P21, H2AX, Bax, Bcl2, caspase6, caspase7, Keap1, Nrf2, Gpx4, TNFa, ATG5, ATG7 mRNA levels of compound **3e** treated Huh-7 cells for 72h. Data are presented as Mean ± SEM. Significant differences were assessed by two-tailed Student's *t*-test. *P<0.05. n = 6.

(Figure 5A). In cells treated with **3e**, the expression of Bcl2, a key gene contributes to apoptosis, increased largely. Moreover, Gpx4 and TNFa, genes involved in oxidative stress, were also increased. The DNA damaged genes and autophagy genes were not changed with **3e** treatment (Figure 5B).

Effects of Compounds 3c and 3e on Protein Expression

In order to further investigate the regulatory role of compounds **3c** and **3e** on the protein expression of the above cell death processes, we treated Huh-7 cells with 10 μM of **3c** and **3e** for 72 h and then the whole cell protein were extracted and detected. After 3c treatment, LC3, the key marker of autophagy, was increased in both conditions (Figure 6A and B). Moreover, H2AX, the protein induced in DNA damage, was significantly increased after **3e** treatment although other proteins had no differences or showed decreased (Figure 6B).

Compounds 3c and 3e Stimulated DNA Damage of Tumor Cells

In order to further verify the effects of compounds **3c** and **3e** on DNA damage, Huh-7 cells were treated with different concentrations (5, 10, 20 μM). After 24 h treatment, cells were analyzed using a DNA damage assay kit. Consistent with the protein expression results, both compounds significantly stimulated DNA damage in a concentration-dependent manner (Figure 7), which may contribute to cell death. This observation strongly supports our mechanistic hypothesis

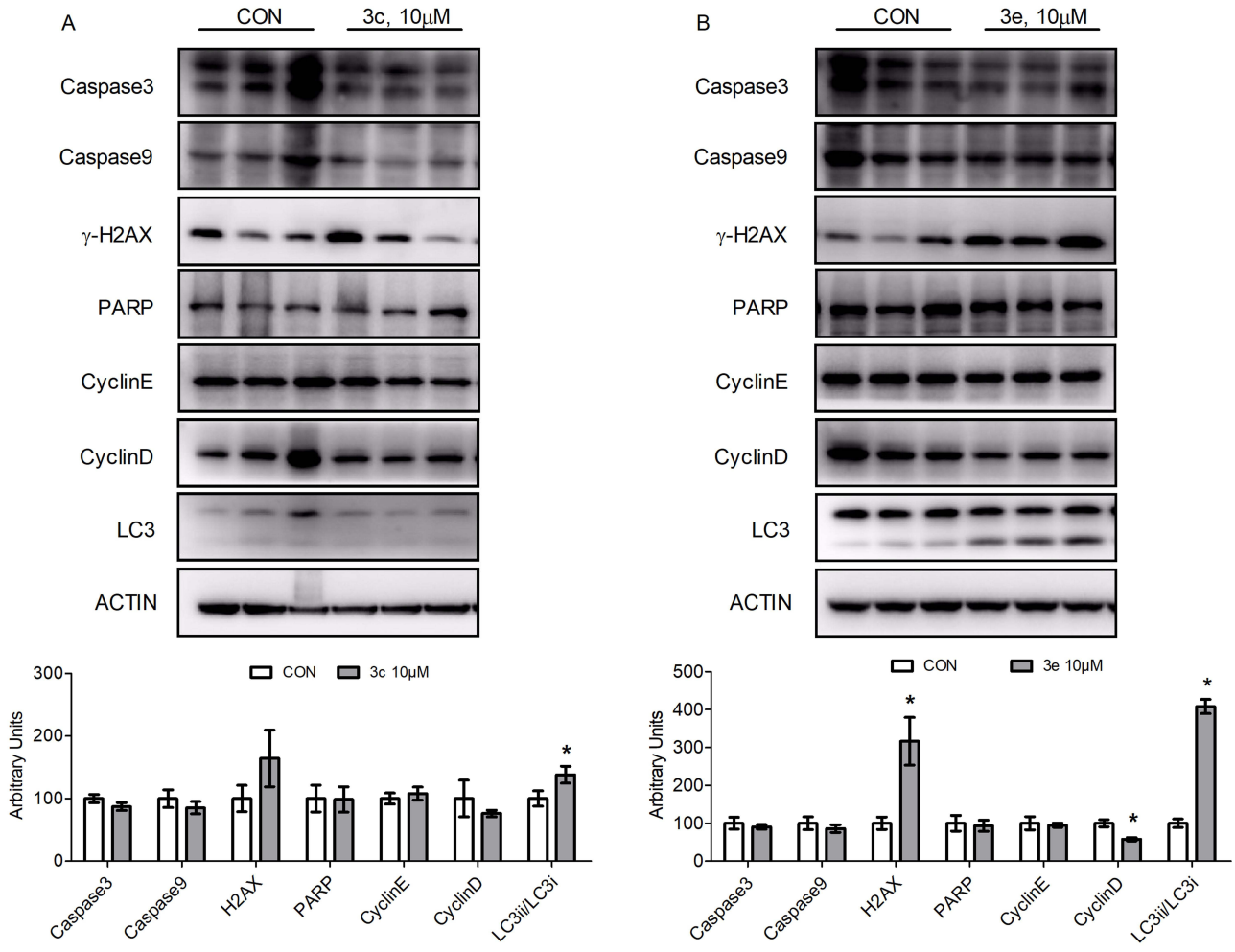

Figure 6 Protein expression analysis. (**A**) Western blot of caspase 3, caspase 9, γ-H2AX, PARP, Cyclin D, Cyclin E, and LC3 in compound **3c** treated Huh-7 cells for 72h. (**B**) Western blot of caspase 3, caspase 9, γ-H2AX, PARP, Cyclin D, Cyclin E, and LC3 in compound **3e** treated Huh-7 cells for 72h. Data are presented as Mean ± SEM. Significant differences were assessed by two-tailed Student's *t*-test. *P<0.05. n = 6.

https://doi.org/10.2147/DDDT.S536920

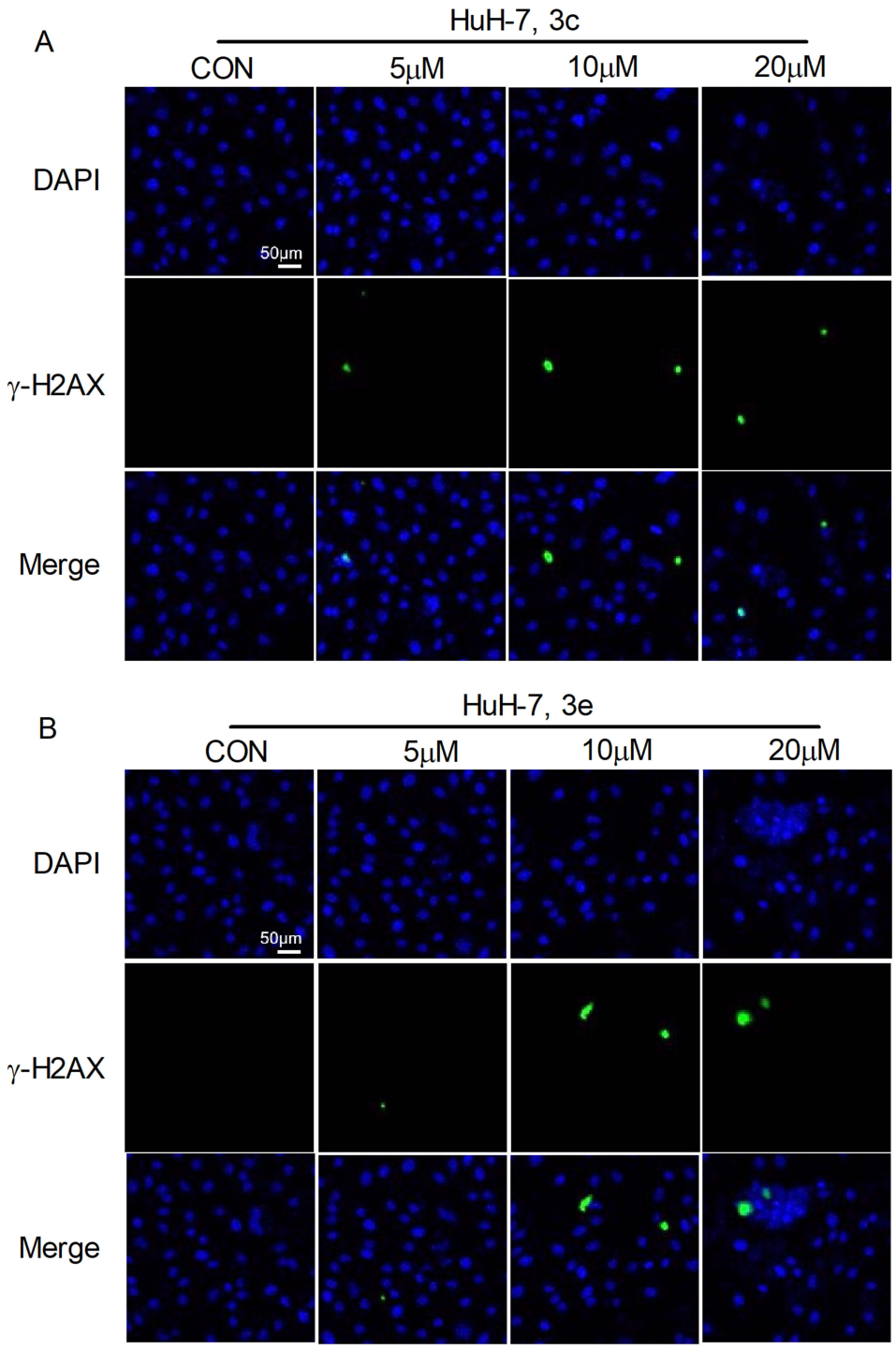

Figure 7 DNA damage detection. (**A**) Huh-7 cells were treated with 5 μM, 10 μM or 20 μM of compound **3c** for 24 h, DNA damaged cells were showed green and the nucleus was showed blue. (**B**) Huh-7 cells were treated with 5 μM, 10 μM or 20 μM of compound **3e** for 24 h, DNA damaged cells were showed green and the nucleus was showed blue, DNA damaged cells were showed green and the nucleus was showed blue. n = 5–6.

that the rigid planar structure of the 1,2,3-triazole-urea hybrids enables DNA intercalation, ultimately leading to DNA damage and cell death. The pronounced effect in Huh-7 cells suggests a potential selectivity, possibly due to the unique molecular features of this hepatocellular carcinoma cell line, such as its dysregulated DNA damage response pathways.

Effects of Compounds 3c and 3e on Autophagy

To evaluate the role of compounds **3c** and **3e** in regulating autophagy, Huh-7 cells were treated with different doses (5, 10, 20 μM) of compounds **3c** and **3e** for 24 h. After treatment, cells were detected by MDC (monodansyl cadaverine) probe, which could specifically label autophagosome and showed green fluorescence. Results showed that autophagosome in tumor cells increased dramatically after compounds **3c** and **3e** treatment (Figure 8). This result indicated that compounds **3c** and **3e** could induce cell autophagy progress in tumor cells, which may finally result in cell death.

Acute Oral Toxicity Assessment

To further assess the safety profile of the compounds, acute toxicity studies were conducted in murine models. Throughout the 14-day observation period, no mortality or significant toxicological manifestations were observed in any experimental groups. Comparative analysis revealed no statistically significant differences in body weight measurements between mice administered with compound **3c** and those in the vehicle control group at all time points. Comprehensive post-mortem examinations, including organ coefficient calculations and histopathological assessments of major organs (cardiac, hepatic, splenic, pulmonary, and renal tissues) demonstrated no detectable toxicological alterations in compound **3c**-treated animals. These collective findings substantiate the favorable safety characteristics of the investigated compounds, thereby providing valuable experimental evidence for evaluating their clinical safety profile, as illustrated in Figure 9.

Conclusion

In this study, we successfully synthesized a novel series of diarylurea and 1,2,3-triazole derivatives through nucleophilic addition and 1,3-dipolar cycloaddition reactions. The compounds demonstrated selective in vitro anticancer activity against multiple tumor cell lines, with particularly potent effects against hepatocellular carcinoma Huh-7 cells. Among the synthesized analogs, compounds **3c** and **3e** emerged as the most promising candidates, exhibiting superior antiproliferative activity against Huh-7 cells, favourable selectivity indexes, and appropriate druggability. Mechanistic studies revealed that these triazole-urea hybrids exert their antitumor effects through multimodal action, including induction of DNA damage, inhibition of cell proliferation, and activation of both apoptotic and autophagic cell death pathways. Besides, the in vivo toxicity measurement demonstrated the safety of the compounds. This research represents the potential of diarylurea-1,2,3-triazole derivatives as therapeutic agents for hepatocellular carcinoma. Our findings not only confirm the therapeutic potential of this chemical scaffold but also provide valuable insights into the development of new anticancer drugs.

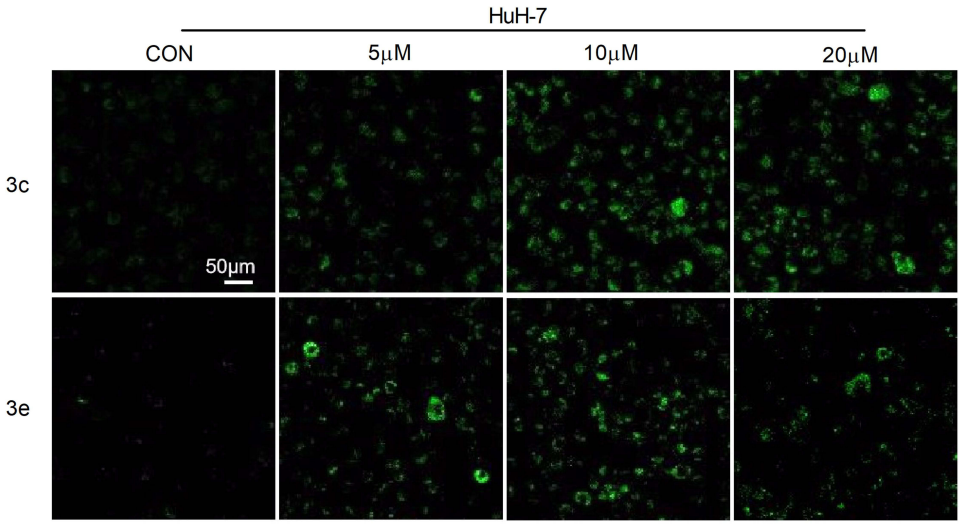

Figure 8 Autophagy measurement. Huh-7 cells were treated with 5 μM, 10 μM or 20 μM of compound **3c** and **3e** for 24 h, autophagy was detected. n = 5–6.

https://doi.org/10.2147/DDDT.S536920

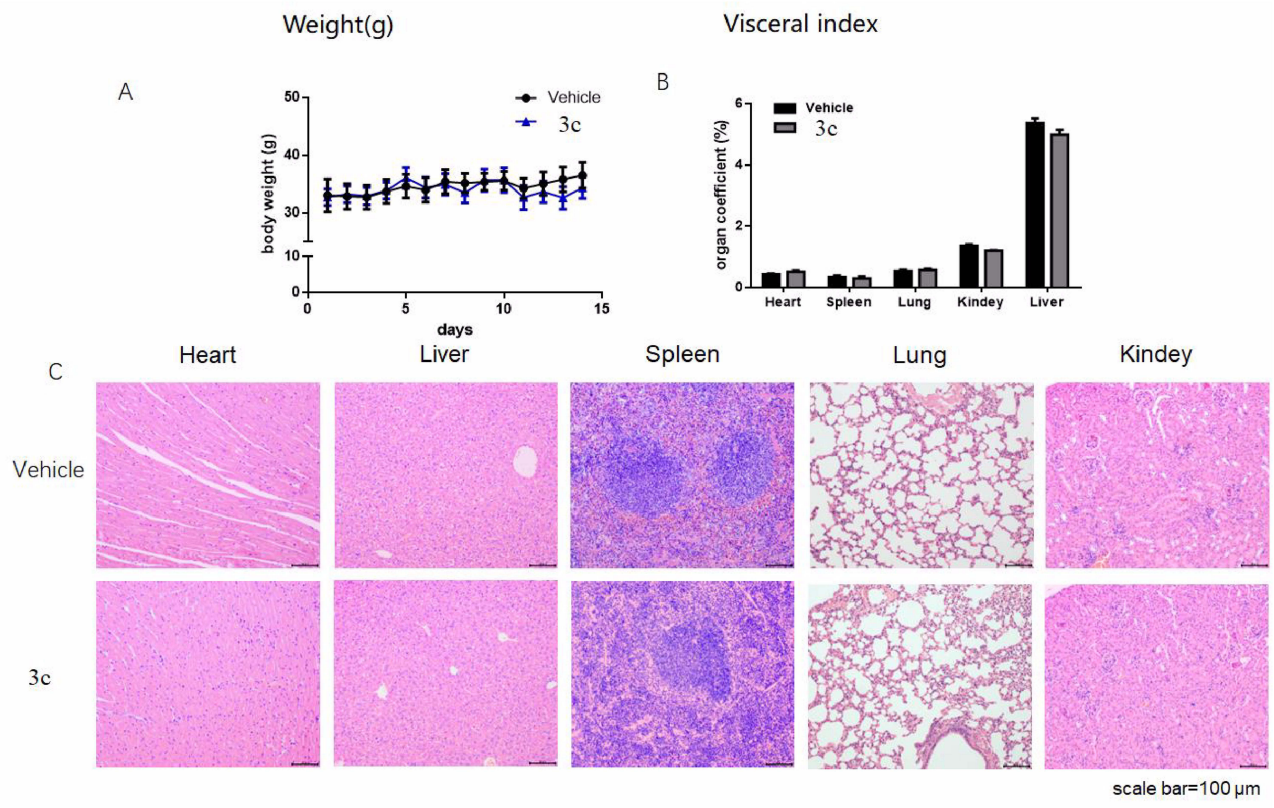

Figure 9 Compound **3c** in vivo toxicity of mice. Acute toxicity experiments of compound **3c** were conducted in mice. (**A**) Mouse body weight changes. (**B**) The acute toxicity experiments examined the effects of compound **3c** on mouse organs (**C**) H&E staining were performed on various organs of mice treated with compound **3c**. n = 5–6. Data are presented as Mean ± SEM. Significant differences were assessed by two-tailed Student's *t*-test. *P<0.05.

Experimental Work

Materials and Chemistry

The 1,2,3-triazole derivative was synthesized in-house by our research group. All the materials involved were purchased from commercial suppliers. Solvents were distilled prior to use. All the reactions were monitored by thin-layer chromatography on 0.25 mm silica gel plates (60GF-254) and visualized with UV light, or chloride ferric. The products were purified by column chromatography, which was performed using 200–300 mesh silica gel. NMR spectra were determined on a Bruker Avance 400 spectrometer, δ in parts per million and J in Hertz. TMS was used as an internal standard. ESI-MS were determined on an API 4000 spectrometer. Measurements were made in DMSO-d_6 solutions. Melting points were tested using an electrothermal melting point apparatus and were uncorrected. The IR spectra were recorded by using Brukar FTIR spectrometer.

The characterization data (^{1}H NMR, ^{13}C NMR, and HRMS) for all compounds are provided in the Supporting Information (Figures S1–S21).

General Procedure for Preparation of Compound 2a (The Method is Suitable for 2b-2c, 4a-4b, 6a-6c)

To a solution of 4-chlorophenyl isocyanate (200 mg, 1.3 mmol) in CH_2Cl_2 (10 mL), 3-aminophenylacetylene (152 mg, 1.3 mmol) was added in one portion. After stirring at room temperature for 2.5 h, the mixture was concentrated, and the residue was purified by column chromatography on silica gel (eluent: PE/EA = 3:1) to make compound **2a** (316 mg, 90%). Mp:212.0–212.4°C. ^{1}H NMR (400 MHz, DMSO-d_6) δ 8.87 (s, 1H), 8.82 (s, 1H), 7.66 (s, 1H), 7.49 (d, J = 8.9 Hz, 2H), 7.40 (d, J = 1.2 Hz, 1H), 7.36–7.27 (m, 3H), 7.09 (dt, J = 7.6, 1.3 Hz, 1H), 4.16 (s, 1H). ^{13}C NMR (100 MHz, DMSO-d_6) δ 152.8, 140.3, 139.0, 129.7, 129.1, 126.0, 125.7, 122.5, 121.5, 120.3, 119.5,

84.0, 80.9. IR (KBr): *v* 3350, 3180 (s, N-H), 2900 (w, C-H), 1680 (vs, C=O str, amide I), 1600 (s, N-H bend, amide II), 1280 (m, C-N str, amide III) cm^{-1}. HR MS (ESI) m/z: calcd for $C_{15}H_{12}ClN_2O$ $[M+H]^+$ 271.0613, found 271.0627.

1-(2-Bromophenyl)-3-(3-Ethynylphenyl)urea (2b)

White solid, yield 85%, Mp:170.0–172.0°C. ^1H NMR (400 MHz, DMSO-d_6) δ 9.57 (s, 1H), 8.17 (s, 1H), 8.05 (dd, J = 8.3, 1.6 Hz, 1H), 7.70 (d, J = 1.9 Hz, 1H), 7.62 (dd, J = 8.0, 1.5 Hz, 1H), 7.46–7.26 (m, 3H), 7.14–7.08 (m, 1H), 6.99 (ddd, J = 8.1, 7.3, 1.6 Hz, 1H), 4.17 (s, 1H).^{13}C NMR (100 MHz, DMSO-d_6) δ 159.1, 153.0, 140.4, 136.3, 129.7, 125.6, 122.5, 121.5, 120.7, 120.6, 119.4, 115.9, 115.7, 84.1, 80.8. IR (KBr): *v* 3280 (s, N-H str), 3080 (w, C-H), 1650 (vs, C=O str, amide I), 1550 (s, N-H bend, amide II), 1250 (m, C-N str, amide III), 650 (m, C-Br str) cm^{-1}. HR MS (ESI) m/z: calcd for $C_{15}H_{12}BrN_2O$ $[M+H]^+$ 315.0128, found 315.0129.

1-(4-Chlorophenyl)-3-(4-Ethynylphenyl)urea (4a)

White solid, yield 86%, Mp:265.5–266.5°C. ^1H NMR (400 MHz, DMSO-d_6) δ 8.90 (d, J = 17.5 Hz, 2H), 7.51–7.45 (m, 4H), 7.41 (d, 2H), 7.34 (d, J = 8.9 Hz, 2H), 4.05 (s, 1H). ^{13}C NMR (100 MHz, DMSO-d_6) δ 152.7, 140.7, 138.9, 132.9, 129.1, 126.0, 120.3, 118.5, 115.2, 84.2, 79.9. IR (KBr): *v* 3250 (s, N-H), 2905 (w, C-H), 1690 (vs, C=O str, amide I), 1660 (s, N-H bend, amide II), 1260 (m, C-N str, amide III) cm^{-1}. HR MS (ESI) m/z: calcd for $C_{15}H_{12}ClN_2O$ $[M+H]^+$ 271.0613, found 271.0640.

1-(2-Bromophenyl)-3-(4-Ethynylphenyl)urea (4b)

White solid, yield 88%, Mp:217.0–218.0°C. ^1H NMR (400 MHz, DMSO-d_6) δ 9.65 (s, 1H), 8.20 (s, 1H), 8.05 (dd, J = 8.3, 1.6 Hz, 1H), 7.63 (dd, J = 8.0, 1.5 Hz, 1H), 7.54–7.46 (m, 2H), 7.43–7.40 (m, 2H), 7.35 (ddd, J = 8.5, 7.3, 1.5 Hz, 1H), 7.00 (td, J = 7.7, 1.6 Hz, 1H), 4.06 (s, 1H). ^{13}C NMR (100 MHz, DMSO-d_6) δ 152.4, 140.6, 137.3, 133.0, 132.9, 128.6, 124.8, 122.9, 118.4, 115.4, 113.8, 84.2, 80.0. IR (KBr): *v* 3260 (s, N-H str), 3160 (w, C-H), 1600 (vs, C=O str, amide I), 1560 (s, N-H bend, amide II), 1270 (m, C-N str, amide III), 655 (m, C-Br str) cm^{-1}. HR MS (ESI) m/z: calcd for $C_{15}H_{12}BrN_2O$ $[M+H]^+$ 315.0128, found 315.0124.

1-(4-Chlorophenyl)-3-(Prop-2-Yn-1-Yl)urea (6a)

White solid, yield 89%, Mp:195.0–196.5°C. ^1H NMR (400 MHz, DMSO-d_6) δ 8.73 (s, 1H), 7.43 (d, J = 8.9 Hz, 2H), 7.27 (d, J = 8.9 Hz, 2H), 6.51 (t, J = 5.7 Hz, 1H), 3.88 (dd, J = 5.7, 2.5 Hz, 2H), 3.11 (s, 1H). ^{13}C NMR (100 MHz, DMSO-d_6) δ 155.1, 139.7, 129.0, 125.3, 119.8, 82.5, 73.3, 29.2. IR (KBr): *v* 3300 (s, C≡C−H), 3190, 3050 (w, Ar-H), 1680 (s, C=O), 1590, 1490, 1450 (m, Ar C=C), 1300 (m, C-N), 750 (m, C-Cl) cm^{-1}. HR MS (ESI) m/z: calcd for $C_{10}H_{10}ClN_2O$ $[M+H]^+$ 209.0476, found 209.0476.

1-(2-Bromophenyl)-3-(Prop-2-Yn-1-Yl)urea (6b)

White solid, yield 86%, Mp:178.4–179.5°C. ^1H NMR (400 MHz, DMSO-d_6) δ 8.03 (dd, J = 8.3, 1.6 Hz, 1H), 7.93 (s, 1H), 7.57 (dd, J = 8.0, 1.5 Hz, 1H), 7.41 (t, J = 5.5 Hz, 1H), 7.29 (ddd, J = 8.5, 7.4, 1.5 Hz, 1H), 6.92 (td, J = 7.6, 1.6 Hz, 1H), 3.92 (dd, J = 5.5, 2.5 Hz, 2H), 3.16 (t, J = 2.5 Hz, 1H). ^{13}C NMR (100 MHz, DMSO-d_6) δ 154.9, 138.0, 132.9, 128.5, 124.0, 122.3, 113.0, 82.1, 73.7, 29.2. IR (KBr): *v* 3350 (s, C≡C−H), 3250, 3050 (w, Ar-H), 1690 (s, C=O), 1690 (m, Ar C=C), 760 (m, C-Br) cm^{-1}. HR MS (ESI) m/z: calcd for $C_{10}H_{10}BrN_2O$ $[M+H]^+$ 252.9971, found 252.9972.

General Procedure for Preparation of Compound 3a

A mixture of compound **2a** (100 mg, 0.37 mmol) and 1-(azidomethyl)-4-chlorobenzene (70 mg, 0.42 mmol) in a mixed solvent of water/tert-butanol/THF (1:1:1, 10 mL) was reacted in the presence of copper sulfate pentahydrate (10 mg, 0.04 mmol) and sodium ascorbate (14 mg, 0.07 mmol) at 85°C. The reaction was monitored by TLC. After completion, the mixture was extracted with dichloromethane (3 × 15 mL). The combined organic layers were washed with water and brine, dried over anhydrous sodium sulfate, and concentrated under reduced pressure. The crude product was purified by column chromatography (DCM/MeOH, 30:1) to afford compound **3a**.

1-(3-(1-(4-Chlorobenzyl)-1H-1,2,3-Triazol-4-Yl)phenyl)-3-(4-Chlorophenyl)urea (3a)

White solid, yield 83%, Mp: 227.5–230.5°C. ^{1}H NMR (400 MHz, DMSO-d_6) δ 8.86 (s, 2H), 8.62 (s, 1H), 8.04 (s, 1H), 7.53–7.22 (m, 11H), 5.66 (s, 2H). ^{13}C NMR (100 MHz, DMSO-d_6) δ 152.9, 147.9,147.8, 140.6, 139.1, 135.5, 133.4, 131.6, 130.4, 129.9, 129.1, 125.9, 122.1, 120.3, 119.5, 118.4, 115.4, 52.7. IR (KBr): v 3435, 3320, 3215 (br, NH and OH), 1705 (vs, C=O), 1605 (m, C=N), 1490 (m, C=C), 1250 (s, C-N), 830 (s, C-Cl) cm^{-1}. HR MS (ESI) m/z: calcd for $C_{22}H_{17}Cl_2N_5NaO$ $[M+Na]^+$ 460.0702, found 460.0763.

1-(3-(1-(3-Chlorobenzyl)-1H-1,2,3-Triazol-4-Yl)phenyl)-3-(4-Chlorophenyl)urea (3b)

White solid, yield 78%, Mp: 217.0–220.0°C. ^{1}H NMR (400 MHz, DMSO-d_6) δ 8.84 (s, 2H), 8.66 (s, 1H), 8.05 (s, 1H), 7.52–7.51 (m, 1H), 7.50–7.49 (m, 1H), 7.48–7.46 (m, 1H), 7.46–7.40 (m, 3H), 7.38–7.30 (m, 5H), 5.67 (s, 2H). ^{13}C NMR (100 MHz, DMSO-d_6) δ 152.9, 147.2, 140.6, 139.1, 138.9, 133.8, 131.6, 131.2, 129.9, 129.1, 128.7, 128.4, 127.2, 125.9, 122.2, 120.3, 119.5, 118.4, 115.4, 52.7. IR (KBr): v 3120 (br, NH and OH), 1710 (vs, C=O), 1665 (m, C=N), 1480 (m, C=C), 1350 (s, C-N), 800 (s, C-Cl) cm^{-1}. HR MS (ESI) m/z: calcd for $C_{22}H_{17}Cl_2N_5NaO$ $[M+Na]^+$ 460.0702, found 460.0763.

1-(3-(1-(4-Bromobenzyl)-1H-1,2,3-Triazol-4-Yl)phenyl)-3-(4-Chlorophenyl)urea (3c)

White solid, yield 79%, Mp: 233.0–236.5°C. ^{1}H NMR (400 MHz, DMSO-d_6) δ 8.84 (s, 2H), 8.61 (s, 1H), 8.04 (d, J = 1.9 Hz, 1H), 7.60 (d, J = 8.4 Hz, 2H), 7.51 (d, J = 8.9 Hz, 2H), 7.47–7.27 (m, 7H), 5.64 (s, 2H). ^{13}C NMR (100 MHz, DMSO-d_6) δ 152.9, 147.2, 140.6, 139.2, 135.9, 133.5, 132.2, 131.6, 130.7, 129.9, 129.19, 125.9, 122.1, 121.9, 120.3, 118.4, 115.4, 52.7. IR (KBr): v 3455, 3265 (br, NH and OH), 1710 (vs, C=O), 1665 (m, C=N), 1590 (m, C=C), 1250 (s, C-N), 750 (m, C-Br) cm^{-1}. HR MS (ESI) m/z: calcd for $C_{22}H_{18}BrClN_5O$ $[M+H]^+$ 482.0378, found 482.0389.

1-(2-Bromophenyl)-3-(3-(1-(4-Chlorobenzyl)-1H-1,2,3-Triazol-4-Yl)phenyl)urea (3d)

White solid, yield 88%, Mp: 206.0–208.0°C. ^{1}H NMR (400 MHz, DMSO-d_6) δ 9.60 (s, 1H), 8.62 (s, 1H), 8.18–7.99 (m, 3H), 7.61 (d, J = 1.5 Hz, 1H), 7.50–7.26 (m, 8H), 6.99 (td, J = 7.6, 1.6 Hz, 1H), 5.66 (s, 2H). ^{13}C NMR (100 MHz, DMSO-d_6) δ 152.6, 147.1, 140.5, 137.5, 135.5, 133.4, 133.0, 131.7, 130.4, 130.0, 129.3, 128.6, 124.6, 122.7, 122.1, 119.6, 118.2,115.2, 113.5, 52.7. IR (KBr): v 3545, 3250 (br, NH and OH), 1715 (vs, C=O), 1675 (m, C=N), 1570 (m, C=C), 820 (s, C-Cl), 750 (m, C-Br) cm^{-1}. HR MS (ESI) m/z: calcd for $C_{22}H_{18}BrClN_5O$ $[M+H]^+$ 482.0378, found 482.0387.

1-(3-(1-(4-Bromobenzyl)-1H-1,2,3-Triazol-4-Yl)phenyl)-3-(2-Bromophenyl)urea (3e)

White solid, yield 85%, Mp: 211.5–213.5°C. ^{1}H NMR (400 MHz, DMSO-d_6) δ 9.61 (s, 1H), 8.62 (s, 1H), 8.17–8.01 (m, 3H), 7.71–7.57 (m, 3H), 7.47–7.25 (m, 6H), 7.00 (dd, J = 7.7, 1.6 Hz, 1H), 5.64 (s, 2H). ^{13}C NMR (100 MHz, DMSO-d_6) δ 152.6, 147.1,144.7, 135.9, 134.9, 133.0, 132.0, 131.7, 130.7, 130.0, 128.6, 124.6, 122.7, 122.1, 121.9, 119.6, 118.2, 115.2, 113.5, 52.7. IR (KBr): v 3340, 3200 (br, NH and OH), 1680 (vs, C=O), 1675 (m, C=N), 1570 (m, C=C), 755 (m, C-Br) cm^{-1}. HR MS (ESI) m/z: calcd for $C_{22}H_{18}Br_2N_5O$ $[M+H]^+$ 525.9873, found 525.9868.

1-(4-(1-(4-Chlorobenzyl)-1H-1,2,3-Triazol-4-Yl)phenyl)-3-(4-Chlorophenyl)urea (5a)

White solid, yield 90%, Mp: 196.5–197.4°C. ^{1}H NMR (400 MHz, DMSO-d_6) δ 8.83 (d, J = 11.9 Hz, 2H), 8.53 (s,1H), 7.76 (d, J = 8.5 Hz, 2H), 7.59–7.42 (m, 6H), 7.42–7.27 (m, 4H), 5.65 (s, 2H). ^{13}C NMR (100 MHz, DMSO-d_6) δ 152.8, 147.2, 139.8, 139.1, 135.5, 130.3, 129.3, 129.2, 129.1, 126.3, 125.9, 124.9, 121.2, 120.2, 119.0, 52.6. IR (KBr): v 3320, 3215 (br, NH and OH), 1705 (vs, C=O), 1605 (m, C=N), 1490 (m, C=C), 1250 (s, C-N), 790 (s, C-Cl) cm^{-1}. HR MS (ESI) m/z: calcd for $C_{22}H_{17}Cl_2N_5NaO$ $[M+Na]^+$ 460.0702, found 460.0763.

1-(4-(1-(3-Chlorobenzyl)-1H-1,2,3-Triazol-4-Yl)phenyl)-3-(4-Chlorophenyl)urea (5b)

White solid, yield 94%, Mp: 195.5–196.5°C. ^{1}H NMR (400 MHz, DMSO-d_6) δ 8.94 (d, J = 11.5 Hz, 2H), 8.57 (s, 1H), 7.76 (d, J = 8.3 Hz, 2H), 7.52 (dd, J = 13.0, 8.6 Hz, 4H), 7.48–7.41 (m, 3H), 7.35–7.27 (m, 3H), 5.67 (s, 2H). ^{13}C NMR (100 MHz, DMSO-d_6) δ 152.9, 147.2, 140.6, 139.2, 138.8, 133.8, 131.2, 129.1, 128.6, 128.3, 127.1, 126.3, 125.8, 124.6, 123.0121.5, 120.2, 119.0, 52.7. IR (KBr): v 3310, 3217 (br, NH and OH), 1735 (vs, C=O), 1615 (m, C=N), 1590 (m, C=C), 1250 (s, C-N), 7950 (s, C-Cl) cm^{-1}. HR MS (ESI) m/z: calcd for $C_{22}H_{17}Cl_2N_5NaO$ $[M+Na]^+$ 460.0702, found 460.0763.

1-(4-(1-(4-Bromobenzyl)-1H-1,2,3-Triazol-4-Yl)phenyl)-3-(4-Chlorophenyl)urea (5c)

White solid, yield 91%, Mp: 238.5–240.6°C. ^{1}H NMR (400 MHz, DMSO-d_6) δ 8.83 (d, J = 11.9 Hz, 2H), 8.53 (s, 1H), 7.76 (d, J = 8.6 Hz, 2H), 7.60 (d, J = 8.4 Hz, 2H), 7.54–7.46 (m, 4H), 7.36–7.16 (m, 4H), 5.63 (s, 2H). ^{13}C NMR (100 MHz, DMSO-d_6) δ 152.8, 147.2, 139.8, 139.1, 135.9, 132.2, 130.6, 129.1, 126.3, 125.9, 124.9, 121.9, 121.3, 120.2, 119.0, 52.7. IR (KBr): v 3540, 3251 (br, NH and OH), 1716 (vs, C=O), 1685 (m, C=N), 1575 (m, C=C),790 (s, C-Cl), 750 (m, C-Br) cm^{-1}. HR MS (ESI) m/z: calcd for $C_{22}H_{18}BrClN_5O$ $[M+H]^+$ 482.0378, found 482.0392.

1-(2-Bromophenyl)-3-(4-(1-(4-Chlorobenzyl)-1H-1,2,3-Triazol-4-Yl)phenyl)urea (5d)

White solid, yield 85%, Mp: 213.5–214.4°C. ^{1}H NMR (400 MHz, DMSO-d_6) δ 9.57 (s, 1H), 8.54 (s, 1H), 8.17 (s, 1H), 8.08 (dd, J = 8.3, 1.6 Hz, 1H), 7.81–7.76 (m, 2H), 7.63 (dd, J = 8.0, 1.5 Hz, 1H), 7.55 (d, J = 8.7 Hz, 2H), 7.47 (d, J = 8.5 Hz, 2H), 7.41–7.30 (m, 3H), 7.00 (dd, J = 7.7, 1.6 Hz, 1H), 5.65 (s, 2H). ^{13}C NMR (100 MHz, DMSO-d_6) δ 152.6, 147.1, 135.5, 133.3,133.2, 133.0, 130.3, 129.3, 128.6, 126.3, 125.0, 124.6, 122.8, 121.3, 121.2, 118.9, 113.6, 52.7. IR (KBr): v 3340, 3261 (br, NH and OH), 1700 (vs, C=O), 1685 (m, C=N), 1575 (m, C=C),795 (s, C-Cl), 755 (m, C-Br) cm^{-1}. HR MS (ESI) m/z: calcd for $C_{22}H_{18}BrClN_5O$ $[M+H]^+$ 482.0378, found 482.0386.

1-(4-(1-(4-Bromobenzyl)-1H-1,2,3-Triazol-4-Yl)phenyl)-3-(2-Bromophenyl)urea (5e)

White solid, yield 76%, Mp: 204.5–206.5°C. ^{1}H NMR (400 MHz, DMSO-d_6) δ 9.57 (s, 1H), 8.54 (s, 1H), 8.17–8.07 (m, 2H), 7.78 (d, J = 8.2 Hz, 2H), 7.65–7.49 (m, 5H), 7.41–7.21 (m, 3H), 6.99 (t, J = 7.7 Hz, 1H), 5.63 (s, 2H). ^{13}C NMR (100 MHz, DMSO-d_6) δ 152.6, 147.1, 139.7, 137.5, 135.9, 133.0, 132.2, 130.6, 128.6, 126.3, 124.9, 124.6, 122.7, 121.9, 121.3, 118.9, 113.7, 52.7. IR (KBr): v 3240, 3255 (br, NH and OH), 1680 (vs, C=O), 1685 (m, C=N), 1575 (m, C=C), 765 (m, C-Br) cm^{-1}. HR MS (ESI) m/z: calcd for $C_{22}H_{18}Br_2N_5O$ $[M+H]^+$ 525.9873, found 525.9864.

1-((1-(4-Chlorobenzyl)-1H-1,2,3-Triazol-4-Yl)methyl)-3-(4-Chlorophenyl)urea (7a)

White solid, yield 88%, Mp: 198.2–199.3°C. ^{1}H NMR (400 MHz, DMSO-d_6) δ 8.70 (s, 1H), 8.03 (s, 1H), 7.43 (dd, J = 10.2, 8.1 Hz, 4H), 7.34 (d, J = 8.5 Hz, 2H), 7.26 (d, J = 8.8 Hz, 2H), 6.63 (s, 1H), 5.58 (s, 2H), 4.32 (d, J = 5.3 Hz, 2H).^{13}C NMR (100 MHz, DMSO-d_6) δ 157.2, 155.4, 139.8, 135.6, 132.4, 133.3, 130.4, 129.2, 128.9, 125.1, 119.6, 52.4, 35.3.

IR(KBr): v 3180 (m, N−H), 1680 (s, C=O), 1600 (m, ArC=C), 1300 (m, C−N), 1050 (m, N−N), 750 (m, C−Cl) cm^{-1}. HR MS (ESI) m/z: calcd for $C_{17}H_{16}C_{l2}N_5$ $[M+H]^+$ 376.0726, found 376.0724.

1-((1-(3-Chlorobenzyl)-1H-1,2,3-Triazol-4-Yl)methyl)-3-(4-Chlorophenyl)urea (7b)

White solid, yield 87%, Mp: 191.5–192.5°C. ^{1}H NMR (400 MHz, DMSO-d_6) δ 8.71 (s, 1H), 8.06 (s, 1H), 7.56–7.36 (m, 5H), 7.30–7.21 (m, 3H), 6.64 (t, J = 5.8 Hz, 1H), 5.60 (s, 2H), 4.33 (d, J = 5.5 Hz, 2H). ^{13}C NMR (100 MHz, DMSO-d_6) δ 155.4, 139.8, 139.0, 133.8, 133.7, 131.2, 128.9, 128.6, 128.3, 127.2, 125.1, 124.5, 119.7, 52.4, 35.3. IR(KBr): v 3170 (m, N−H), 1580 (s, C=O), 1605 (m, ArC=C), 1300 (m, C−N), 1050 (m, N−N), 780 (m, C−Cl) cm^{-1}. HR MS (ESI) m/z: calcd for $C_{17}H_{16}C_{l2}N_5$ $[M+H]^+$ 376.0726, found 376.0725.

1-((1-(4-Bromobenzyl)-1H-1,2,3-Triazol-4-Yl)methyl)-3-(4-Chlorophenyl)urea (7c)

White solid, yield 79%, Mp: 197.5–198.6°C. ^{1}H NMR (400 MHz, DMSO-d_6) δ 8.70 (s, 1H), 8.02 (s, 1H), 7.58 (d, J = 8.4 Hz, 2H), 7.42 (d, J = 8.9 Hz, 2H), 7.30–7.20 (m, 4H), 6.63 (t, J = 5.6 Hz, 1H), 5.56 (s, 2H), 4.32 (d, J = 5.6 Hz, 2H). ^{13}C NMR (100 MHz, DMSO-d_6) δ 164.0, 155.4, 139.8, 136.0, 132.1, 130.7, 128.9, 125.1, 123.3, 121.9, 119.6, 52.4, 35.3. IR(KBr): v 3165 (m, N−H), 1680 (s, C=O), 1605 (m, ArC=C), 1310 (m, C−N), 1050 (m, N−N), 760 (m, C−Cl) cm^{-1}. HR MS (ESI) m/z: calcd for $C_{17}H_{16}BrClN_5O$ $[M+H]^+$ 420.0221, found 420.0221.

1-(2-Bromophenyl)-3-((1-(4-Chlorobenzyl)-1H-1,2,3-Triazol-4-Yl)methyl)urea (7d)

White solid, yield 87%, Mp: 205.5–206.5°C. ^{1}H NMR (400 MHz, DMSO-d_6) δ 8.13–8.01 (m, 2H), 7.92 (s, 1H), 7.59–7.49 (m, 2H), 7.49–7.41 (m, 2H), 7.35 (d, J = 8.4 Hz, 2H), 7.28 (t, J = 7.9 Hz, 1H), 6.90 (td, J = 7.6, 1.6 Hz, 1H), 5.60 (s, 2H), 4.34 (d, J = 5.5 Hz, 2H). ^{13}C NMR (100 MHz, DMSO-d_6) δ 172.9, 155.1, 138.2, 135.6, 133.3, 132.8, 130.4, 129.2, 128.4, 123.8, 123.5, 122.1, 112.7, 52.4, 35.3. IR(KBr): v 3180 (m, N−H), 1675 (s, C=O), 1580 (m, ArC=C), 1310 (m, C−N), 1050 (m, N−N) cm^{-1}. HR MS (ESI) m/z: calcd for $C_{17}H_{16}BrClN_5O$ $[M+H]^+$ 420.0221, found 420.0227.

1-((1-(4-Bromobenzyl)-1H-1,2,3-Triazol-4-Yl)methyl)-3-(2-Bromophenyl)urea (7e)

White solid, yield 85%, Mp: 188.6–188.7°C. ^{1}H NMR (400 MHz, DMSO-d_6) δ 8.08–8.00 (m, 2H), 7.92 (s, 1H), 7.61–7.47 (m, 4H), 7.32–7.25 (m, 3H), 6.90 (t, J = 7.2 Hz, 1H), 5.57 (s, 2H), 4.34 (d, J = 5.6 Hz, 2H). ^{13}C NMR (100 MHz, DMSO-d_6) δ 155.2, 138.7, 138.1, 136.0, 132.8, 132.1, 130.7, 128.4, 123.9, 122.1, 121.9, 118.2, 112.8, 52.5, 35.3. IR(KBr): v 3170 (m, N−H), 1680 (s, C=O), 1620 (m, ArC=C), 1305 (m, C−N), 1150 (m, N−N), 760 (m, C-Br) cm^{-1}. HR MS (ESI) m/z: calcd for $C_{17}H_{16}Br_2N_5O$ $[M+H]^+$ 463.9716, found 463.9715.

Biological Study

Dimethylsulfoxide (DMSO) was obtained from Sigma-Aldrich (St. Louis, Missouri, USA). Dulbecco's modified Eagle medium (DMEM), RPMI 1640 Medium, Fetal bovine serum (FBS) and penicillin/streptomycin were brought from Gibco (Grand Island, NY, USA). Enhanced Cell Counting Kit-8, Calcein/PI Live/Dead Viability Assay Kit, DNA damage detection kit, and Autophagy Staining Assay kit were bought from Beyotime Biotechnology (Shanghai, China). Annexin V-FITC/Propidium iodide (PI) staining kit was provided by BD Biosciences (Franklin Lake, New Jersey, USA).

Cell Culture

Lung cancer cell lines H460, H1299, A549, PC-9, hepatocellular carcinoma cell line Huh-7, breast cancer cell line MCF-7, and L02 cells were obtained from ATCC. Cells were cultured using DMEM or RPMI 1640 added with 10% FBS and 1% penicillin/streptomycin. Cells were incubated in a humidified atmosphere with 5% CO_2 at 37°C.

Cell Viability and IC_{50} Measurement

CCK8 assay kit was used to measure cell viability. Cells were seeded in a 96-well plate with the density of 3×10^3 cells/well. After adhere overnight, cells were treated with 20 μM or 50 μM of the compounds or vehicle control DMSO dissolved in culture media for 48 h or 72h. Then, the CCK8 reagent was added, and cells were incubated for another 1 hour at 37°C with 5% CO_2. Cells were measured using a microplate spectrophotometer (Thermo) at 450nm absorbance. Cell viability was calculated as a percentage relative to the control group. To determine IC_{50} values, cells treated with different concentrations (0, 10 μM, 20 μM, 40 μM, 80 μM) of the compounds for 72 h. The inhibition percentage of cells was calculated using cell viability, and the IC_{50} value was calculated using GraphPad Prism software. The sample size in CCK-8 assay was more than 5 in each group. The results were expressed as Mean ± SE, data were analyzed using one-way analysis of variance (ANOVA) followed by Dunnett's tests. $P < 0.05$ were considered statistically significant.

Live and Dead Cell Staining

HuH-7 cells were seeded in 96-well plates with a density of 3×10^3 cells/well. After overnight incubation, cells were treated with different doses (0, 5 μM, 10 μM, 20 μM) of the compounds. After 24 h treatment, a LIVE/DEAD Assay Kit was used to dye the living and dead cells, and observed by fluorescent microscope. The number of replicates was 5–6 in each group.

Apoptosis Assay

HuH-7 cells at a density of 3×10^5 cells/well were cultured in 6-well plates. After adhesion overnight, cells were treated with different doses (0, 5 μM, 10 μM, 20 μM) of compounds for 72h. Then, cells were collected and stained using Annexin V-FITC and propidium iodide. The apoptotic ratio was quantified using the flow cytometry (BD Biosciences) and analyzed by FlowJo software v10. Values were expressed as Mean ± SE. Statistical significance was assessed using one-way analysis of variance (ANOVA) followed by Dunnett's tests. $P < 0.05$ was considered statistically significant. Data were performed using GraphPad Prism. The number of replicates was 5–6 in each group.

RT-PCR Measurement

Huh-7 cells were seeded in a 12-well plate and treated with compounds (10 μM) for 72h. Total RNA was extracted using TRIzol reagent (Ambion, USA), and RT-PCR was performed using PowerUp TM SYBRTM Green Master Mix (ABI, USA). Gene expression was normalized to GAPDH. Primers were obtained from Sangon Biotech (Shanghai, China) and are listed in Table 5. Values were expressed as Mean ± SEM. Statistical significance was assessed using a two-tailed Student's t-test. $P < 0.05$ was considered statistically significant. The number of replicates was 6 in each group.

Table 5 List of Oligonucleotide Primer Pairs Used in RT-PCR Analysis

Gene	Forward Primer (5'-3')	Reverse Primer (5'-3')
P53	CCTCAGCATCTTATCCGAGTGG	TGGATGGTGGTACAGTCAGAGC
P21	AGGTGGACCTGGAGACTCTCAG	TCCTCTTGGAGAAGATCAGCCG
H2AX	CGGCAGTGCTGGAGTACCTCA	AGCTCCTCGTCGTTGCGGATG
Bax	TCAGGATGCGTCCACCAAGAAG	TGTGTCCACGGCGGCAATCATC
Bcl2	ATCGCCCTGTGGATGACTGAGT	GCCAGGAGAAATCAAACAGAGGC
Caspase3	GGAAGCGAATCAATGGACTCTGG	GCATCGACATCTGTACCAGACC
Caspase6	AGGTGGATGCAGCCTCCGTTTA	ATGAGCCGTTCACAGTTTCCCG
Caspase7	CGGAACAGACAAAGATGCCGAG	AGGCGGCATTTGTATGGTCCTC
Keap1	CAACTTCGCTGAGCAGATTGGC	TGATGAGGGTCACCAGTTGGCA
Nrf2	AGGTTGCCCACATTCCCAAA	ACGTAGCCGAAGAAACCTCA
Gpx4	TTGGTCGGCTGGACGAGG	GGGACGCGCACATGGT
Tnfa	ACTGAAAGCATGATCCGGGACG	AGCAGGCAGAAGAGCGTGGTGG
ATG5	GGATGGGATTGCAAAATGACAGA	TCCTAGTGTGTGCAACTGTCC
ATG7	GGCCAATAAGATGGGTCTGA	GCTTTTGTCCACTGCTCCTC

Western Blot Measurement

Protein expressions were analyzed using Western blotting. HuH-7 cells were cultured in 12-well plates and treated with compounds (10 μM) for 72h. Whole cell proteins were extracted using radioimmunoprecipitation assay (RIPA) buffer containing protease/phosphatase inhibitor cocktail (CST). Antibodies used were as followed, caspase3, caspase9, γH2AX, PARP, cyclin D, cyclin E, LC3), and β-actin (all from CST). Values were expressed as Mean ± SEM. Statistical significance was assessed using a two-tailed Student's *t*-test. $P < 0.05$ was considered statistically significant. Data were performed using GraphPad Prism. The number of replicates was 6 in each group.

DNA Damage Staining

Huh-7 cells with a density of 3×10^3 cells/well were seeded in 96-well plates. Different doses (0, 5μM, 10μM, 20μM) of the compounds were added to cells for 24h. DNA damage detection Kit was used to dye the cells, cell nucleus was stained by blue, and DNA damaged cells were stained by green. Then, cells were observed and photographed by a fluorescent microscope. The number of replicates was 5–6 in each group.

Autophagy Staining Assay

Huh-7 cells were seeded in a 96 well plate at the density of 3×10^3 cells/well. Cells were treated with compounds at the doses of 0, 5μM, 10μM, and 20μM. After 24h treatment, the medium was removed, and cells were stained with monodansylcadaverine (Beyotime Biotechnology, Shanghai, China) for 1 hour in dark at 37°C. Then, cells were photographed with a confocal microscopy. The number of replicates was 5–6 in each group.

In vivo Assay

Animals

SPF-grade healthy Kunming mice (8 weeks old) were purchased from Henan Skbex Biotechnology Co., Ltd (Licence No.: SCXK (Yu) 2020–0005). The experiment adhered to the 3R principle of "reduction, replacement, optimization", aiming to minimize the harm and suffering of animals to the greatest extent possible. Mice were kept under a 12-hour light/dark cycle and provided with free access to drinking water and were acclimated to the feeding conditions for 7 days.

After acute toxicity test, mice were sacrificed by intraperitoneal administration of pentobarbital dissolved in sterile saline at a dose of 150mg/kg body weight. The animal study was reviewed and approved by The Ethics Committee for the Care and Use of Laboratory Animals of Henan University of Science and Technology (Approval number: HAUST-024-M081001, Approval data: October 17th, 2024).

Acute Toxicity Test

Female KM mice at 8 weeks of age were randomly divided into the following groups: vehicle control group, **3c**-treated group. Each group had 6 mice. Mice in the vehicle control groups were given an equivalent volume of vehicle (5% DMSO + 40% PEG300 + 1% Tween 80 + 54% saline) by intragastric administration, while mice in the **3c**-treated groups were given the **3c** solution (500 mg/kg). Body weight and appearance were monitored for a total period of 14 days (from the first day after treating with **3c**). The representative organs (heart, liver, spleen, lungs, and kidneys) were harvested, and weighed to calculate the organ coefficient (organ coefficient = organ weight/body weight × 100%). Then, the organs were fixed in 10% formaldehyde and paraffin-embedded for histological examination. Finally, these sections were stained with haematoxylin and eosin (H&E) for light microscopic examination. Data were analyzed using Student's *t*-test and $P < 0.05$ was considered statistically significant.

Statistical Analyses

We performed statistical analyses using GraphPad Prism 9.5 software, these data were analyzed using one-way analysis of variance (ANOVA) followed by Dunnett's tests for the comparisons of multiple groups or Student's *t*-test for the comparisons of two groups. Data were obtained from no fewer than three independent experiments. A *p*-value less than 0.05 was considered statistically significance.

Data Sharing Statement

The data underlying this study are available in the published article and its Supporting Information.

Ethics Statement

The animal study was reviewed and approved by The Ethics Committee for the Care and Use of Laboratory Animals of Henan University of Science and Technology. All methods are reported in accordance with ARRIVE guidelines and in accordance with the relevant guideline and regulation. The animal experiment adhered to the 3R principle of "reduction, replacement, optimization" and The Ethics Committee for the Care and Use of Laboratory Animals of Henan University of Science and Technology, aiming to minimize the harm and suffering of animals to the greatest extent possible.

Funding

This work was supported by the Tackle Key Problems in Science and Technology Project of Henan Province, China (Grant No. 242102311222 and 242102311226). The Scientific Research Foundation for PhD (Henan Normal University, NO. 5101039170343 and Xinxiang University, NO. 1366020232), Futian Healthcare Research Project (No. FTWS2023068), Shenzhen Science and Technology Program (ZDSYS20220606100801004).

Disclosure

The authors declare that they have no conflicts of interest.

References

1. Siegel RL, Miller KD, Jemal A. Cancer Statistics, 2017. *CA-A Cancer J Clin*. 2017;67(1):7–30. doi:10.3322/caac.21387
2. Sung H, Ferlay J, Siegel RL, et al. Global cancer statistics 2020: GLOBOCAN estimates of incidence and mortality worldwide for 36 cancers in 185 countries. *CA-A Cancer J Clin*. 2021;71(3):209–249. doi:10.3322/caac.21660
3. Chen S, Cao Z, Prettner K, et al. Estimates and projections of the global economic cost of 29 cancers in 204 countries and territories from 2020 to 2050. *JAMA Oncol*. 2023;9(Bray4):465–472. doi:10.1001/jamaoncol.2022.7826
4. Shabbits JA, Krishna R, Mayer LD. Molecular and pharmacological strategies to overcome multidrug resistance. *Expert Rev Anticancer Therapy*. 2001;1(4):585–594. doi:10.1586/14737140.1.4.585
5. Kurt Yilmaz N, Schiffer CA. Introduction: drug resistance. *Chem Rev*. 2021;121(6):3235–3237. doi:10.1021/acs.chemrev.1c00118

6. Wu J, Lin Z. Non-small cell lung cancer targeted therapy: drugs and mechanisms of drug resistance. *Int J Mol Sci*. 2022;23(23):15056. doi:10.3390/ijms232315056
7. Zhao S, Liu J, Lv Z, Zhang G, Xu Z. Recent updates on 1,2,3-triazole-containing hybrids with *in vivo* therapeutic potential against cancers: a mini-review. *Eur J Med Chem*. 2023;251:115254. doi:10.1016/j.ejmech.2023.115254
8. Bozorov K, Zhao J, Aisa HA. 1,2,3-Triazole-containing hybrids as leads in medicinal chemistry: a recent overview. *CA-A Cancer J Clin*. 2019;27(16):3511–3531. doi:10.1016/j.bmc.2019.07.005
9. Guan Q, Xing S, Wang L, et al. Triazoles in medicinal chemistry: physicochemical properties, bioisosterism, and application. *J Med Chem*. 2024;67(10):7788–7824. doi:10.1021/acs.jmedchem.4c00652
10. Bonandi E, Christodoulou MS, Fumagalli G, Perdicchia D, Rastelli G, Passarella D. The 1,2,3-triazole ring as a bioisostere in medicinal chemistry. *Drug Discovery Today*. 2017;22(10):1572–1581. doi:10.1016/j.drudis.2017.05.014
11. Ronchetti R, Moroni G, Carotti A, Gioiello A, Camaioni E. Recent advances in urea- and thiourea-containing compounds: focus on innovative approaches in medicinal chemistry and organic synthesis. *Rsc Med Chem*. 2021;12(7):1046–1064. doi:10.1039/d1md00058f
12. Li H-Q, Lv P-C, Yan T, Zhu H-L. Urea derivatives as anticancer agents. *Anti-Cancer Agents Med Chem*. 2009;9(4):471–480. doi:10.2174/1871520610909040471
13. Pinheiro Pd SM, Franco LS, Montagnoli TL, Fraga CAM. Molecular hybridization: a powerful tool for multitarget drug discovery. *Expert Opinion Drug Discovery*. 2024;19(4):451–470. doi:10.1080/17460441.2024.2322990
14. Gontijo VS, Dias Viegas FP, Cristancho Ortiz CJ, et al. Molecular hybridization as a tool in the design of multi-target directed drug candidates for neurodegenerative diseases. *Curr Neuropharmacol*. 2020;18(5):348–407. doi:10.2174/1385272823666191021124443
15. Alkhzem AH, Woodman TJ, Blagbrough IS. Design and synthesis of hybrid compounds as novel drugs and medicines. *RSC Adv*. 2022;12(30):19470–19484. doi:10.1039/D2RA03281C
16. Ivasiv V, Albertini C, Goncalves AE, Rossi M, Bolognesi ML. Molecular hybridization as a tool for designing multitarget drug candidates for complex diseases. *Curr Top Med Chem*. 2019;19(19):1694–1711. doi:10.2174/1568026619666190619115735
17. Bakale RD, Bhagat AN, Mhetre UV, et al. Design, synthesis and molecular docking study of novel quinoline–triazole molecular hybrids as anticancer agents. *J Mole Struct*. 2025;1321:140072. doi:10.1016/j.molstruc.2024.140072
18. Mhetre UV, Bhagat AN, Londhe SV, et al. Quinazolinone-linked triazole conjugates: synthesis, biological evaluation, and in silico studies. *J Mole Struct*. 2025;1331:141594. doi:10.1016/j.molstruc.2025.141594
19. Ma L-Y, Wang B, Pang L-P, et al. Design and synthesis of novel 1,2,3-triazole-pyrimidine-urea hybrids as potential anticancer agents. *Bioorg Med Chem Lett*. 2015;25(5):1124–1128. doi:10.1016/j.bmcl.2014.12.087
20. Egile C, Kenigsberg M, Delaisi C, et al. the selective intravenous inhibitor of the MET tyrosine kinase SAR125844 inhibits tumor growth in MET-amplified cancer. *Mol Cancer Ther*. 2015;14(2):384–394. doi:10.1158/1535-7163.mct-14-0428
21. Hsu K-L, Tsuboi K, Chang JW, et al. Discovery and optimization of piperidyl-1,2,3-triazole ureas as potent, selective, and *in vivo*-active inhibitors of α/β-hydrolase domain containing 6 (ABHD6). *J Med Chem*. 2013;56(21):8270–8279. doi:10.1021/jm400899c
22. Duan Y-C, Zheng Y-C, Li X-C, et al. Design, synthesis and antiproliferative activity studies of novel 1,2,3-triazole-dithiocarbamate-urea hybrids. *Eur J Med Chem*. 2013;64:99–110. doi:10.1016/j.ejmech.2013.03.058
23. Hou X, Gong X, Mao L, Zhao J, Yang J. Discovery of Novel 1,2,3-triazole Derivatives as IDO1 Inhibitors. *Pharmaceuticals*. 2022;15(11):1316. doi:10.3390/ph15111316
24. Gao E, Wang Y, Fan G-L, et al. Discovery of gefitinib-1,2,3-triazole derivatives against lung cancer via inducing apoptosis and inhibiting the colony formation. *Sci Rep*. 2024;14(1):9223. doi:10.1038/s41598-024-60000-1
25. Liu ZJ, Liu JC, Gao E, Mao LF, Hu S, Li SQ. Synthesis and *in vitro* antitumor activity evaluation of gefitinib-1,2,3-triazole derivatives. *Molecules*. 2024;29(4). doi:10.3390/molecules29040837